

Inelastic Response of RC Moment Resisting Frames with URM Infills

Archanaa Dongre

Ph D Scholar, IIT Hyderabad, India

Ramancharla Pradeepkumar

Associate Professor, IIT Hyderabad, India



ABSTRACT:

Brick masonry type of construction is found all over India and neighbouring countries like Nepal and Bangladesh. In India, these buildings are commonly found in North, extending from Punjab to West Bengal and Central India, from Haryana to Madhya Pradesh. These buildings are most commonly found in regions where good quality clay for brick production is abundantly available (World housing encyclopaedia report, 2003). But, past earthquakes witness major loss to brick masonry type of buildings. Many analytical and experimental studies have been done in past to understand the behaviour of brick masonry buildings during earthquake. Analytical study mainly includes, numerical modelling of the brick masonry buildings of type URM and Reinforced concrete Infill wall.

In this work, primary focus is given to numerical modelling and nonlinear behaviour of brick masonry buildings subjected to lateral loads and understanding crack propagation in wall and calculation of quantitative damage to the building in terms of stiffness, ductility in load displacement curve.

Keywords: RC framed brick infill, numerical modelling, stiffness, strength

1. INTRODUCTION

RC framed brick infill type of construction is widely used in most of the Asian countries but past earthquakes witness enormous loss to human life and property due to collapse of brick masonry buildings. Though framed structures with masonry infill are commonly used in regions of high seismicity but adequate knowledge of the behavior is required to design this type of structure in order to reduce the loss of life and property associated with a possible structural failure. Most of the rural India has construction of load bearing structures such as stone masonry, unreinforced brick masonry and confined masonry buildings which are lacking the seismic safety measures suggested by seismic code, so it becomes important to assess the behavior of such building under seismic loading.

Past study shows that numerical modeling of such buildings helped to understand the behavior during earthquake. For the analysis of masonry buildings basically three approaches need to be considered. i.e., detailed micro modeling, simplified micro modeling and macro modeling. Detailed micro modeling considers the two components of masonry, brick and mortar separately. The interface represents a potential crack/slip plane with initial dummy stiffness to avoid interpretation of the continuum (Lourenco, 1996). This approach provides detailed insight of the structural behavior but it is computationally costly (Paola, 2006). In the second approach, mortar and brick properties are considered as combined and so brick masonry thus considered as a set of elastic blocks bonded by potential fracture/slip lines at the joints. In this approach, brick arrangement is kept as input variable of the analysis and therefore walls with discontinuities such as windows and door openings can be analyzed (L. Gambarotta, 1996 and Lourenco, 1996). The third approach is macro modeling, it uses homogenization techniques which considers masonry as a periodic media i.e. elements arranged in uniform pattern. Two stages of homogenization are used, one for the orthotropic material and the other for smeared cracking of the material (Lofti et al, 1994). Macro models are capable to analyze large structures, but it cannot consider discontinuities and details.

In this study, inelastic response of RC moment resisting framed with un-reinforced masonry infills is considered. Four cases are considered in order to understand the capacity of bare frame and infill wall

with and without consideration of reinforcement. A monotonic load has been considered under displacement control and a base shear versus drift ration relation has been plotted and effect of loading on strength and stiffness of the wall has been studied.

2. NUMERICAL ANALYSIS FOR RC MOMENT RESISTING FRAMES WITH URM INFILLS

2.1 Applied Element Method (AEM)

In AEM, structure is assumed to be virtually divided into small square elements each of which is connected by pairs of normal and shear springs set at contact locations with adjacent elements. These springs bear the constitutive properties of the domain material in the respective area of representations (Figure 1). Global stiffness of structure is built up with all element stiffness contributed by that of springs around corresponding element. Global matrix equation is solved for three degrees of freedom of these elements for 2D problem. Stress and strain are defined based on displacement of spring end points of element edges. Details of Applied Element scheme can be found in literatures by Meguro et al (1998).

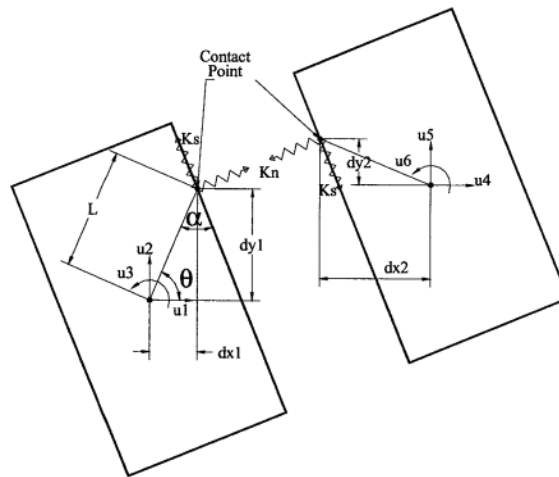


Figure 1. Element shape, contact point and degrees of freedom

2.2 Discretization for Brick Masonry:

Anisotropy of the masonry is accounted by considering masonry as a two phase material with brick units and mortar joint set in a regular interval. Structure is discretized such that each brick unit is represented by a set of square elements where mortar joints lie in their corresponding contact edges (see Figure 2).

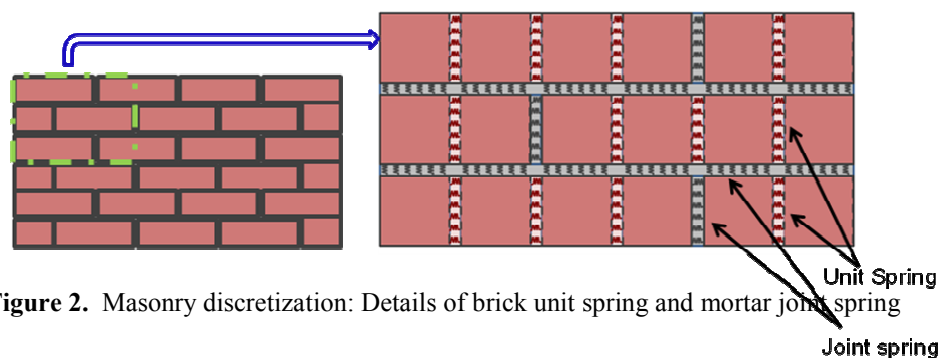


Figure 2. Masonry discretization: Details of brick unit spring and mortar joint spring

In spring level, springs that lie within one unit of brick are termed as 'unit springs'. For those springs, the corresponding domain material is brick as isotropic nature and they are assigned to structural

properties of brick. Springs those accommodate mortar joints are treated as ‘joint springs’. They are defined by equivalent properties based on respective portion of unit and mortar thickness.

Figure 2 shows the configuration of brick units, joints and their representation in this study. The initial elastic stiffness values of joint springs are defined as in Eq. 1.1 and 1.2 (Bishnu, 2004).

$$K_{nunit} = \frac{E_u t d}{a}; \quad K_{njoint} = \frac{E_u E_m t d}{E_u \times t_h + E_m (a - t_h)} \quad (1.1)$$

$$K_{sunit} = \frac{G_u t d}{a}; \quad K_{sjoint} = \frac{G_u G_m t d}{G_u \times t_h + G_m (a - t_h)} \quad (1.2)$$

Where E_u and E_m are Young’s modulus for brick unit and mortar, respectively, whereas G_u and G_m are shear modulus for the same. Thickness of wall is denoted by ‘t’ and ‘t_h’ is mortar thickness. Dimension of element size is represented by ‘a’ and ‘d’ is the fraction part of element size that each spring represent. While assembling the spring stiffness for global matrix generation, contribution of all springs around the structural element are added up irrespective to the type of spring. In the sense, for global solution of problem, there is no distinction of different phase of material but only their corresponding contribution to the stiffness system.

2.3 Masonry material model

Material model used was a composite model that takes into account of brick and mortar with their respective constitutive relation with elastic and plastic behavior of hardening and softening. Brick springs were assumed to follow principal stress failure criteria with linear elastic behavior. Once there is splitting of brick reaching elastic limit, normal and shear stress are assumed not to transfer through cracked surface in tensile state. The brick spring’s failure criterion is based on a failure envelope given by Eq. 3:

$$\frac{f_b}{f'_b} + \frac{f_t}{f'_t} = 1 \quad (1.3)$$

Where f_b and f_t are the principal compression and tensile stresses, respectively, and f'_b and f'_t are the uniaxial compression and tensile strengths, respectively.

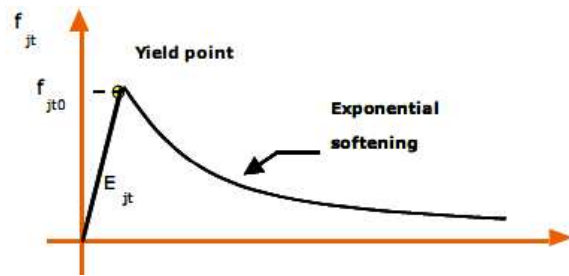
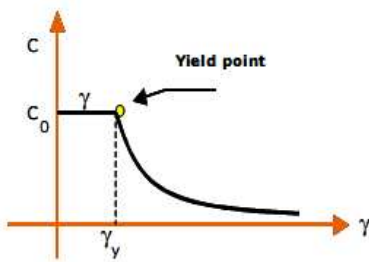


Figure 3. Cohesion degradation (Bishnu Pandey, 2002) **Figure 4.** Bond degradation (Bishnu Pandey, 2002)

Coulomb’s friction surface with tension cut-off is used as yield surface after which softening of cohesion and maximum tension takes place in exponential form as a function of fracture energy values and state variables of damage. The cohesion and bond values are constant till the stress first time when stress exceeds the respective failure envelopes. Figure 3 and 4 show the degradation scheme of bond and cohesion. Failure modes that come from joint participation of unit and mortar in high compressive stress is considered by liberalized compression cap as shown in Figure 5. The effective masonry compressive stress used for cap mode follows hardening and softening law as shown in Figure 6.

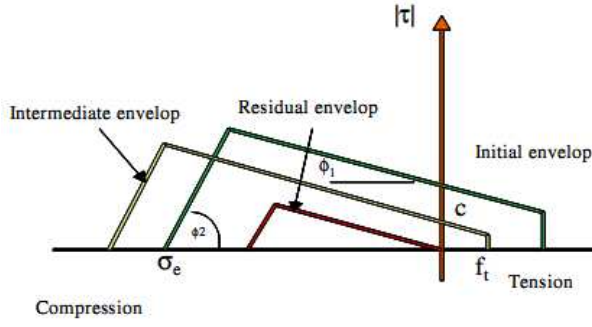


Figure 5. Failure criteria for joint spring (Sutcliffe et al, 2001) (Lourenco, 1996)

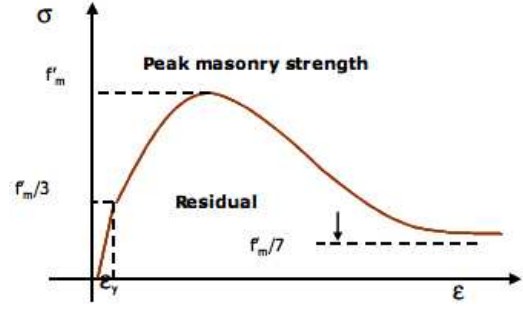


Figure 6. Hardening and softening applied for joint spring in compression cap (Lourenco, 1996)

The tension cut-off, f_t , and the sliding along joints, f_2 , exhibit softening behavior whereas the compression cap experiences hardening at first and then softening. The failure surfaces used in this study derived from Lourenço, (1996), with some simplification are as given in Eqs. (1.4), (1.5) and (1.6). (Figure 5)

$$f_1(\sigma, K_1) = \sigma - f_t \exp\left(-\frac{f_t}{G_f^I} K_1\right) \quad (1.4)$$

$$f_2(\sigma, K_2) = |\tau| + \sigma \tan(\phi_1) - c \exp\left(-\frac{c}{G_f^{II}} K_2\right) \quad (1.5)$$

$$f_3(\sigma, K_3) = |\tau| + \sigma \tan(\phi_2) \{(\sigma_3(K_3) - \sigma)\} \quad (1.6)$$

In above equations, K_1 , K_2 and K_3 are hardening and softening parameters for tension, shear and compression behavior respectively. G_f^I and G_f^{II} is fracture energy in tension and shear respectively.

2.4 Material Model for Concrete and Steel:

As a material modeling of concrete under compression condition, Maekawa compression model [Okamura and Maekawa, 1991], as shown in Figure 7(a), is adopted. The tangent modulus is calculated according to the strain at the spring location and whether the spring is in loading or unloading process. For more details, refer to [Okamura and Maekawa, 1991]. After reaching the peak compression stresses, stiffness is assumed as a minimum value (1% of initial value) to avoid having a singular stiffness matrix. The difference between calculated spring stress and stress corresponding to the strain at the spring location are redistributed each increment. And for shear springs, model shown in Figure 7(b) is assumed. Till the cracking point stresses are assumed to be proportional to strains and after that stiffness is assumed as minimum value (1% of initial value) to avoid having a singular stiffness matrix. For reinforcement, bilinear stress strain relation is assumed. After yield of reinforcement, steel spring stiffness is assumed as 1% of the initial stiffness as shown in Figure 7(c). No model is used, up to this stage, for cut of reinforcement because the behavior of the structure becomes mainly dynamic behavior and the static stiffness matrix becomes singular.

It should be emphasized that some other failure phenomena, like buckling of reinforcement and spalling of concrete cover, are not considered in the analysis in this analysis. However, the shear transfer and shear softening are approximately considered in the analysis. For more details about material models used and the results in case of monotonic loading conditions, refer to [Meguro and Tagel-din, 2001]

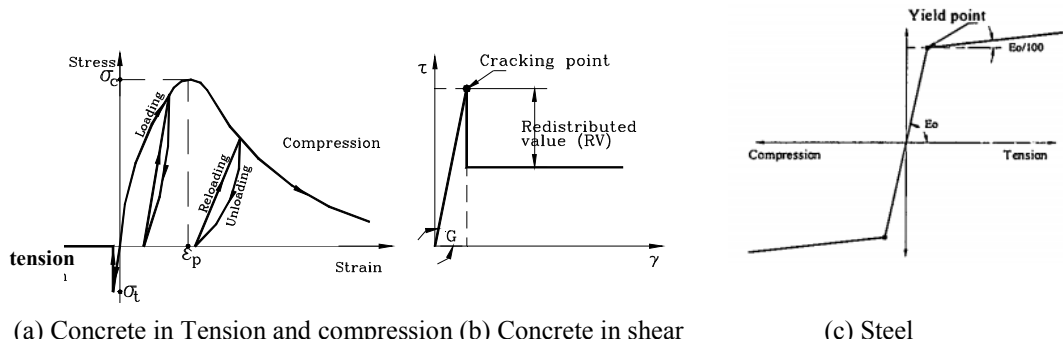


Figure 7. Material models for concrete (Okamura and Maekawa, 1991) and steel

2.5 Failure Criteria

One of the main problems associated with the use of elements having three degrees of freedom is the modeling of diagonal cracking. Applying Mohr-Coulomb's failure criteria calculated from normal and shear springs, not based on principal stresses, has some problems. When the structure is really composed of individual elements, such as granular material or brick masonry buildings, Mohr-Coulomb's failure criteria is reasonable. The idea of the present technique is how to use the calculated stresses around each element to detect the occurrence of cracks. To determine the principal stresses at each spring location, the following technique is used.

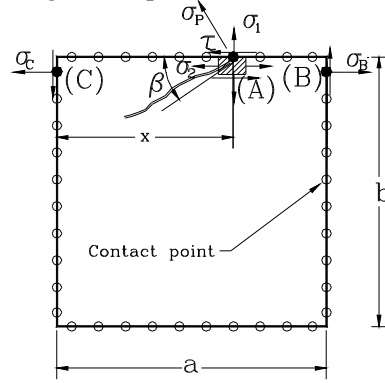


Figure 8. Failure Criteria

Referring to Figure 8, the shear and normal stress components (τ and σ_1) at point (A) are determined from the normal and shear springs attached at the contact point location. The secondary stress (σ_2) can be calculated by Eq. 1.7 from normal stresses in points (B) and (C), as shown in Figure 8.

$$\sigma_2 = \frac{x}{a} \sigma_B + \frac{(a-x)}{a} \sigma_C \quad (1.7)$$

The principal stress calculated as in Eq. 1.8:

$$\sigma_p = \left(\frac{\sigma_1 + \sigma_2}{2} \right) + \sqrt{\left(\frac{\sigma_1 - \sigma_2}{2} \right)^2 + (\tau)^2} \quad (1.8)$$

The value of principal stress (σ_p) is compared with the tension resistance of the studied material. When σ_p exceeds the critical value of tension resistance, the normal and shear spring forces are redistributed in the next increment by applying the normal and shear spring forces in the reverse direction. These redistributed forces are transferred to the element centre as a force and moment, and then these redistributed forces are applied to the structure in the next increment. The redistribution of spring forces at the crack location is very important for following the proper crack propagation. For the normal spring, the whole force value is redistributed to have zero tension stress at the crack faces. Although shear springs at the location of tension cracking might have some resistance after cracking

due to the effect of friction and interlocking between the crack faces, the shear stiffness is assumed zero after crack occurrence.

Referring to Figure 8, local crack inclination angle (β) to the element edge direction can be calculated as follows in Eq. 1.9:

$$\tan(2\beta) = \left(\frac{2\tau}{\sigma_1 + \sigma_2} \right) \quad (1.9)$$

Having zero value of shear stress means that the crack direction is coincident with the element edge direction. In shear dominant zones, the crack direction is mainly dominant by shear stress value. This technique is simple and has the advantage that no special treatment is required representing the cracking. In cases when the shear stresses are not dominant, like case of slender frames, the angle (β) tends to be zero. This indicates that the crack is parallel to the element edge and hence, high accuracy is expected.

2.6 Modeling of Wall Frame Interface and Numerical Scheme

Interface between wall and RC frame has been treated basically as mortar interface between brick units. Mortar joint constitutive law for tension, compression and shear as described in previous section has been implemented. Normal stiffness of interface spring has been derived as that of equivalent spring from series of brick, mortar and adjoining concrete element participating to one spring. However, elastic shear stiffness is taken of that mortar component assuming weaker shear plane for cracking is passed through the interface not in the brick and concrete component. Failures of interface spring in tension represent the detaching of the panel from frame shear sliding between panel and frame is represented by friction developed in large displacement range.

2. UNDERSTANDING CAPACITY OF BARE FRAME AND INFILL WALL WITH AND WITHOUT CONSIDERATION OF REINFORCEMENT

In this study four cases have been considered (Figure 9). Geometry, boundary conditions and loading as given below:

- i. Bare frame with no reinforcement
- ii. Bare frame with longitudinal and transverse reinforcement
- iii. Infill wall with no reinforcement in frame
- iii. Infill wall with longitudinal and transverse reinforcement in frame

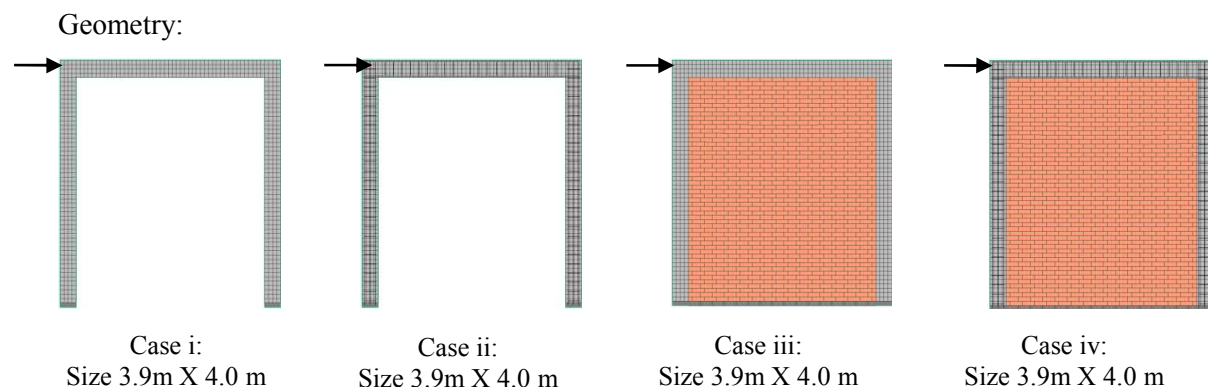


Figure 9. Cases considered for the study

Boundary conditions: Base elements are considered as fixed

Loading conditions: Displacement control used. For all the above cases a displacement of 10mm has been applied in 100 increments and its response is plotted as base shear versus drift ratio.

Reinforcement Details:

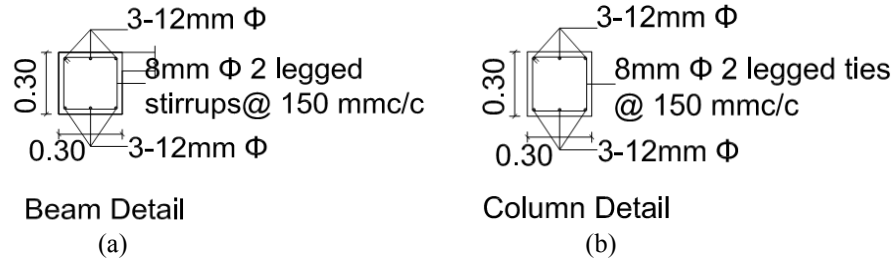


Figure 10. Reinforcement details for (a) Beam (b) Column

To understand the effect of reinforcement above four cases have been considered. In first case, frame with no transverse or longitudinal reinforcement whereas in second case frame is considered with longitudinal and transverse reinforcement and its effect is seen in Figure 11 (a) as explained below. Third case is the combination of first case but with brick infill and fourth case is combination of 2nd case with brick infill which is in actual construction practice. Effect of the reinforcement and infill can be seen in Figure 11 (b)

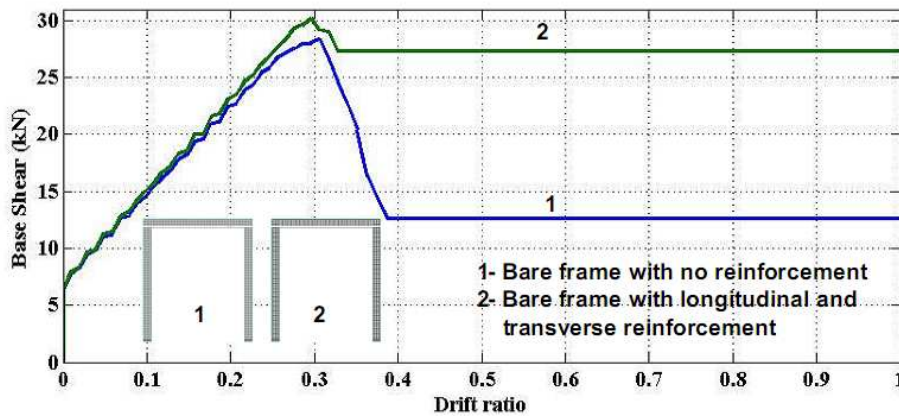


Figure 11. (a) Base shear versus drift ratio for bare frames

Figure 11 (a) shows the base shear versus drift ratio for the first two cases, bare frame with no reinforcement and bare frame with longitudinal and transverse reinforcement. Effect of initial stiffness can be observed for both the cases. Till the peak yield point both the frames are capable to take lateral load whereas frame with reinforcement is showing more load carrying capacity with high stiffness when compared with the first case. After the yield, effect of reinforcement plays major role, as for case 2, strength degradation is very less and frame shows a good ductile behavior whereas for case 1, strength degradation is rapid and load carrying capacity decreased drastically when compared with case 2, this is due to presence of reinforcement which is giving high stiffness and ductility to the frame.

Figure 11 (b) shows the base shear versus drift ratio for the last two cases, i.e. case 3 of brick infill with no reinforcement in frame and case 4 as brick infill with longitudinal and transverse reinforcement in frames. It can be seen that effect of reinforcement initially very less i.e. negligible when both the cases compared, this is due to the presence of infill wall which is increasing overall stiffness of the system till the yielding. After yielding effect of reinforcement can be clearly seen, as considerable stiffness and strength degradation with less ductility can be observed in case 3 when compared with case 4.

In order to quantify strength versus stiffness for infill as well as bare frame, at first individual cases has been considered. Figure 12 shows the strength versus stiffness of bare frame. It can be observed that at initial stages frame is having high stiffness which is reducing with the load increment. i.e., stiffness of the bare frame is initially minimum for high initial strength of frame but as strength starts degrading stiffness of frame settles at around 90000 kN/m for frame strength of 8 kN.

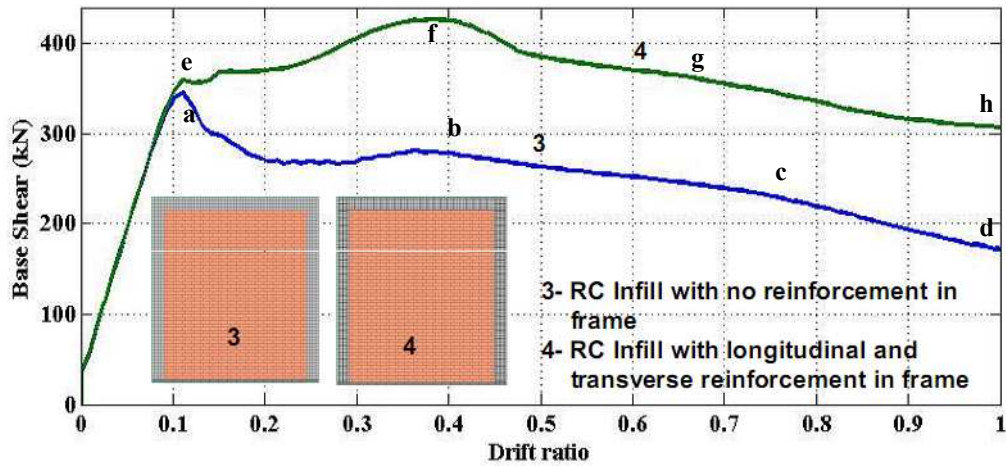


Figure 11. (b) Base shear versus drift ratio for RC Infill wall

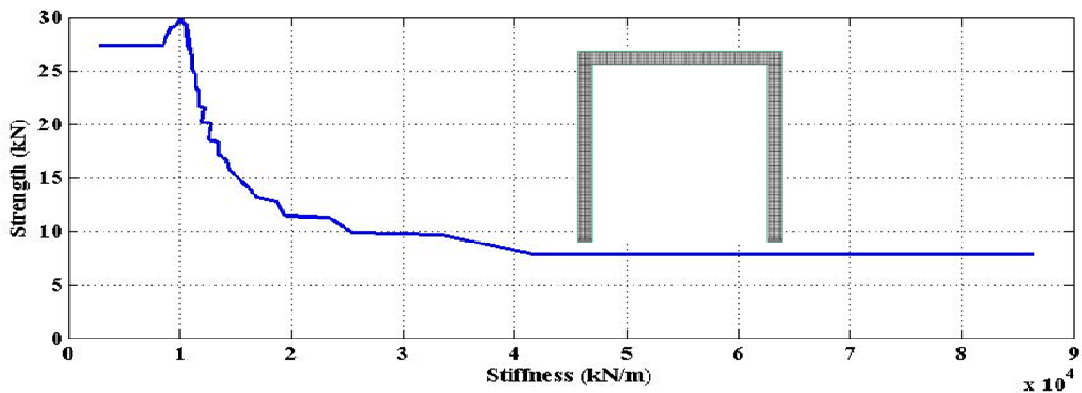


Figure 12. Strength versus stiffness of bare frame

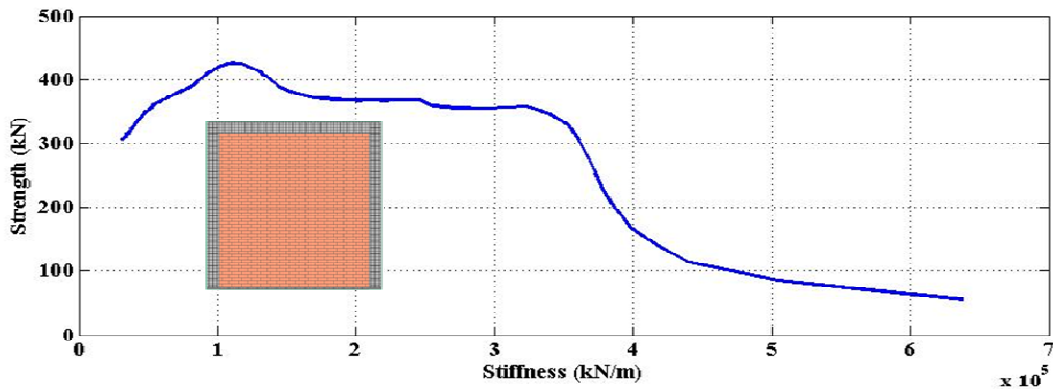


Figure 13. Strength versus stiffness of Infill wall

Figure 13 clearly shows the effect of infill wall on overall strength of the wall, wall shows high load carrying capacity above 350 kN till the stiffness of 350000 kN/m but later stages of loading strength starts degrading but wall still carries a stiffness of 630000 kN/m.

Range of shift in stiffness for bare frame and infill:

Figure 14 shows the stiffness versus displacement applied for bare frame and infill wall, a clear shift in stiffness can be observed in curve 1 and curve 2 with respect to the displacement applied on structure. This increase in stiffness in curve 1 is due to the addition of infill wall in frame increased the stiffness of wall considerably.

A ratio of stiffness of infill and stiffness of bare frame is plotted in Figure 15 with respect to displacement applied. Initially this ratio is continuously increasing; at peak (point 1) is 24 at 0.0014m

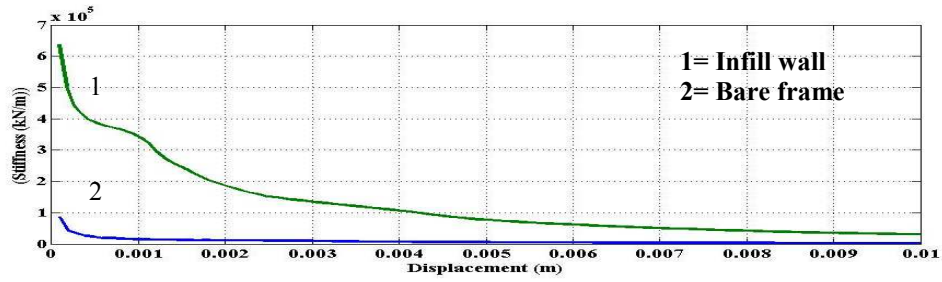


Figure 14 Stiffness versus displacement for bare frame and Infill wall

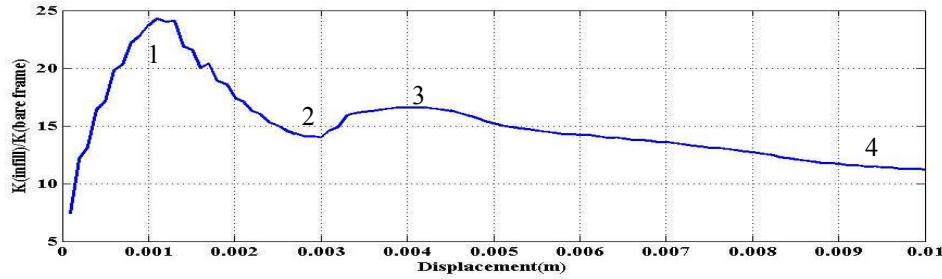


Figure 15. Stiffness ratios versus displacement for bare frame and Infill wall

displacement, whereas with increase in displacement, ratio is coming down till point 2 on curve, but from point 2 to 3 there is slight increase in ratio due to the effect of infill but from point 3 to 4 is decreasing continuously with increase in displacement. Figure 16 shows the ratio of strength of infill to the bare frame. Similar behavior can be observed as discussed in Figure 15. Figure 17 is plotted to get the combined effect of Figure 15 and 16. Behavior in Curve 1 is explained in Figure 15 whereas Curve 2 shows similar behavior as in Curve 1.

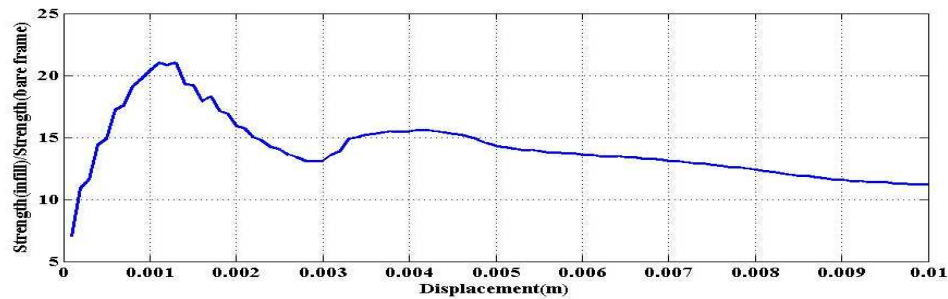


Figure 16. Strength ratios versus displacement(m) for bare frame and Infill wall

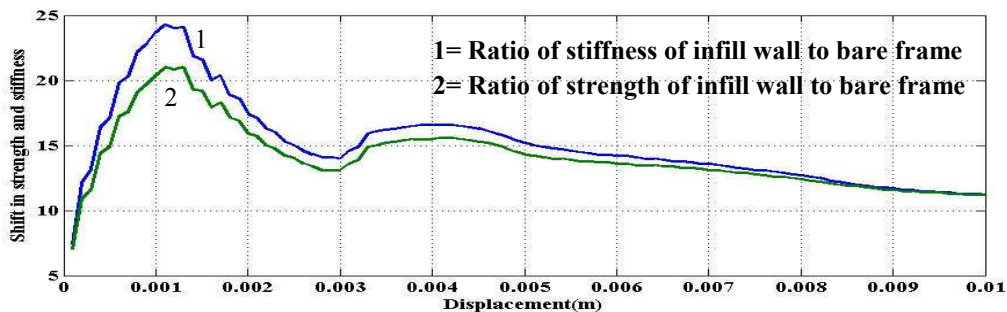


Figure 17. Comparison of shift in strength and stiffness for bare frame and Infill wall

2.1 Damage Quantification: Damage to the building depends on strength, stiffness and ductility of the building. It can be written as in Eq. 2.1 and computed on the basis of base shear and drift ratio curve

$$D = f(\text{strength, stiffness and ductility}) \quad (2.1)$$

Damage is considered on the scale of 0 to 1, where 0 means no damage and 1 mean total collapse of the building. For example, consider Figure 11(b), for curve no. 3, At point 'a' on the curve, at 0.11 drift ratio, stiffness and strength degradation can be seen this is due to initiation of cracks in brick wall; so at point 'a' damage can be identified as 0.1. From point 'a' to 'b' due to absence of reinforcement in frame these cracks are continuously increasing and stiffness and strength degradation is in progress. Though cracks are increasing but still wall is able to carry good amount of load (230kN), so at point 'b' damage can be indicated as 0.4, at point 'c' to 'd' there is still more decrease in strength and stiffness due to load increment and cracks are widening but still wall is stable so at point 'c' damage can be indicated as 0.6 and at point 'd' damage is indicated as 0.7 where considerable cracks have been developed and retrofitting should be done.

For curve no. 4, at point 'e' crack initiation started but due to closing and opening of cracks, though stiffness is decreasing but increase in strength can be observed. At point 'e' damage can be indicated as 0.1 at point 'f' though increase in strength but decrease in stiffness can be seen, so damage can be indicated as 0.2. Similarly, at point 'g' damage indicated as 0.3 with slight decrease in load carrying capacity and at point 'h' damage is 0.4 as wall is still stable enough and can carry more load.

3. CONCLUSION:

In this study, behavior of different types of structures has been studied with the effect of reinforcement. Full advantage of applied element method has been taken which is capable to capture initiation of crack in the structure till the total collapse of the structure. The four cases specifically can be divided in two parts of frame without infill and with infill. In first part a frame is considered but with and without any reinforcement and in second part with and without reinforcement in columns and beams. The last case of RC framed brick infill clearly comes out to be the most effective in terms of strength, stiffness and ductility of the structure. A RC framed infill wall of case 4 shows almost 13 times more load carrying capacity than that of RC frame of case 2.

Damage quantification is done on the basis of drift ratio versus base shear curve, depends on stiffness, strength and ductility of the curve. RC framed infill wall shows a good ductile behavior with good strength and stiffness due to which damage to the wall is minimum.

REFERENCES:

- Bishnu Pandey et al, "Simulation of brick masonry wall behavior under in-plane lateral loading using Applied Element method", 13th World Conference on Earthquake Engineering, Canada, 2004
- J.G. Rots, "Numerical simulation of cracking in structural masonry", Project under Computational Masonry Mechanics, 1991
- L. Gambarotta and S. Lagomarsino, "Damage models for the seismic response of brick masonry shear walls", Part1: The mortar joint model and its applications (1996), Part2: The continuum model and its applications, 1996
- Lofti, H.R. Shing, "Interface model applied to fracture of masonry structures", J. structure eng., ASCE, 120(1), 63-80, 1994
- Lourenco P. B., "Computational strategies for masonry structures", Ph. D. Dissertation, Delft University of Technology, Delft, The Netherlands, 1996
- Meguro K. and Hakuno M. (1989), "Fracture analyses of structures by the modified distinct element method", Structural Eng./Earthquake Eng., Japan Society of Civil Engineers, Vol. 6. No. 2, pp. 283s-294s.
- Okamura, H. and Maekawa, K., "Nonlinear analysis and constitutive models of reinforced concrete, Gihodo Co. Ltd., Tokyo, 1991
- Paola Mayorca, "Report on the state – of-the art in the seismic retrofitting of unreinforced masonry houses by PP-Band meshes", 2006
- Sutcliffe DJ, Yu H.S, Page AW. "Lower Bound Limit Analysis of Unreinforced Masonry Shear Walls." Computer & Structures 2001; (79):1295-1312
- Tagel-Din Hatem and Meguro (2001), A new efficient method for nonlinear, large deformation and collapse analysis of structures